Title:

Greater distal activation of the biceps femoris long head reflects proximodistal differences in motor unit action potential properties.

Authors:

José Carlos dos Santos Albarello[1], Hélio V. Cabral[2], Francesco Negro[2,#], Liliam Fernandes de Oliveira[1,#]

[#]These authors contributed equally to this work and shared senior authorship.

Affiliations:

[1]Biomedical Engineering Program (COPPE), Universidade Federal do Rio de Janeiro, Rio de Janeiro, Brazil.

[2]Department of Clinical and Experimental Sciences, Università degli Studi di Brescia, Brescia, Italy.

Acknowledgements:

This study was funded by CAPES, FAPERJ and FINEP. We would like to thank Dr. Taian Vieira for his valuable feedback on the manuscript, which helped us refine the terminology and enhance the interpretation of our findings.

Corresponding authors:

Dr. Hélio V. Cabral

Department of Clinical and Experimental Sciences

Università degli Studi di Brescia

Viale Europa 11, Brescia, 25121, Italy

Email: helio.daveigacabral@unibs.it

Abstract

Purpose: Recent research has explored region-specific responses within the biceps femoris long head. However, evidence on regional muscle activation remains controversial, primarily because information derived solely from surface electromyograms (sEMG) amplitude does not necessarily provide an accurate estimate of neural drive to the muscle. To address this limitation, this study investigated whether there are proximodistal differences in motor unit properties of the biceps femoris long head during isometric hip extension and knee flexion tasks. **Methods:** Seventeen resistance-trained males performed isometric knee flexion and hip extension tasks at 20% and 40% of maximal voluntary contraction. High-density sEMG were recorded from proximal and distal regions of the biceps femoris long head and decomposed into individual motor units. Central motor unit properties (mean discharge rate, discharge rate variability, recruitment and de-recruitment thresholds) and action potential properties (amplitude and conduction velocity) were analyzed. Bipolar sEMG amplitude was also calculated for each region to simulate traditional sEMG measurements. **Results:** Bipolar sEMG amplitude, motor unit action potential amplitude and conduction velocity were significantly greater in the distal region during both tasks. In contrast, no proximodistal differences were observed in central motor unit properties. **Conclusion:** These findings suggest that increased bipolar sEMG amplitude in the distal region of the biceps femoris long head is driven by motor unit action potential properties rather than differences in central modulation, likely influenced by intra-muscular variations in muscle mechanics and geometry. This emphasizes limitations of relying solely on sEMG amplitude to infer neural control strategies in the biceps femoris long head.

Keywords: hamstrings, high-density surface EMG; neural drive, regional activation.

Introduction

Predominantly composed of biarticular muscles (apart from the biceps femoris short head), the hamstrings play a key role in tasks requiring hip extension and knee flexion movements and are therefore engaged in many daily living activities (Afonso et al. 2021; Kellis and Blazevich 2022). For instance, during the leg swing phase in running or sprinting, the hamstrings contract eccentrically to decelerate the hip flexion and knee extension, thereby greatly contributing to the stabilization of these joints during directional changes (Fields et al. 2005; Hogervorst and Vereecke 2015). However, the substantial eccentric load at the end of the swing phase, when the hamstrings are at longer lengths, makes this muscle group highly susceptible to stretch-induced injuries, particularly during high-velocity movements (Jonhagen et al.; Liu et al. 2012; Danielsson et al. 2020; Jokela et al. 2023). Indeed, the incidence of hamstring injuries in sports has systematically increased over the last years (Ekstrand et al. 2023), with still high prevalence rates (Zachazewski et al. 2019; Ribeiro-Alvares et al. 2020). Despite significant efforts by the scientific community to understand the underlying mechanisms and develop strategies for prevention and treatment (Brukner 2015), the rate of hamstring injuries has remained relatively unchanged over the past 30 years (Maniar et al. 2022). This persistent trend underscores the need for further research to address existing gaps in this literature, aiming to reduce the risk of hamstrings injuries.

Of particular interest, a wide body of research has recently explored region-specific responses within the hamstring muscles, particularly in the proximal and distal regions of the biceps femoris long head (Schoenfeld et al. 2015; Watanabe et al. 2016; Hegyi et al. 2019), which is the most frequently injured muscle among the hamstrings (Opar et al., 2012). The possibility of a proximodistal selective response in the biceps femoris long head during hip extension and knee flexion tasks primarily arises from existing evidence suggesting task-dependent regional activation in biarticular muscles (Watanabe et al. 2021), such as the rectus femoris (Miyamoto et al. 2012;

Watanabe et al. 2012) and the gastrocnemius (Wolf et al. 1993; Cohen et al. 2020) muscles. However, evidence regarding the biceps femoris long head muscle remains controversial. For instance, Watanabe et al. (2016) observed no differences in the proximodistal activation of the biceps femoris long head muscle during knee flexion and hip extension isometric tasks. Conversely, Hegyi et al. (2019) reported greater activation in the distal region compared to the proximal region during the hamstring curl exercise (which exclusively involves knee flexion) but found no proximodistal differences during hip extension exercises. These inconsistent findings may be attributed to the fact that information extracted solely from the amplitude of surface electromyograms (sEMG) does not necessarily provide an accurate estimate of the neural drive to the muscle due to a phenomenon known as "amplitude cancellation" (Keenan et al. 2005; Farina et al. 2010). Moreover, sEMG amplitude is also influenced by various peripheral factors, such as muscle architecture and motor unit conduction velocity (Farina et al. 2004, 2014), further complicating the interpretation of changes in sEMG amplitude as changes in the neural drive to the muscle (Martinez-Valdes et al. 2018).

These limitations can be overcome by combining blind source separation methods with high-density surface electromyogram (HDsEMG) recordings, which allow for the noninvasive decomposition and assessment of the activity of individual motor units (Holobar and Zazula 2007; Negro et al. 2016). These methods enable the direct study of central and peripheral properties of motor units located in different muscles or muscle regions (Martinez-Valdes et al. 2018; Valli et al. 2024), providing a more precise estimate of potential proximodistal differences in the control of the biceps femoris long head muscle. Therefore, in this study, we investigated whether there are proximodistal differences in the motor unit properties of the biceps femoris long head during hip extension and knee flexion isometric tasks. To achieve this, we decomposed motor unit spike trains from HDsEMG acquired from the proximal and distal regions of the biceps femoris long head and

compared central (mean discharge rate, discharge rate variability, recruitment threshold and de-recruitment threshold) and action potential (motor unit conduction velocity and motor unit action potential amplitude) properties between regions. Additionally, to compare our findings with proximodistal differences in bipolar sEMG, as previously reported (Schoenfeld et al. 2015), we simulated two bipolar sEMG detection sites in the proximal and distal regions and calculated their amplitude, both normalized and non-normalized.

Methods

Participants

Seventeen healthy men (mean ± SD; age: 30 ± 4 years; height: 176.82 ± 6.09 cm; body mass: 84.71 ± 10.46 kg) participated in this study. All participants were resistance training practitioners and reported no lower limb musculoskeletal injuries in the preceding 6 months. Prior to the start of experiments, all participants read and signed an informed consent form. The study was conducted in accordance with the latest version of the Declaration of Helsinki and was approved by the ethics committee of the Clementino Fraga Filho University Hospital of the Federal University of Rio de Janeiro (approval number: 6.259.296).

Experimental protocol

All experimental procedures were carried out in a single visit to the laboratory lasting approximately 90 minutes. Initially, participants were familiarized with the equipment and tasks, followed by measurements of body mass and height. Then, participants were asked to perform isometric torque-matching tasks involving knee flexion and hip extension contractions (**Figure 1A**). For the knee flexion task, participants lay prone on the dynamometer chair, with the knee joint axis aligned as coaxially as possible with the dynamometer's axis of rotation (left panel in

Figure 1A). For the hip extension task, participants stood on the shaft of the dynamometer, aligning the hip joint as coaxially as possible with the dynamometer's axis of rotation (right panel in **Figure 1A**). These positions were chosen to maintain the biceps femoris at approximately the same muscle length between conditions.

Each task followed the same experimental protocol (bottom part of **Figure 1A**). First, participants performed two maximum voluntary isometric contractions (MVC) for 5 seconds, with a 30-second interval between contractions. The highest value from the two MVCs was considered for the subsequent submaximal isometric tasks. After a 2-minute rest, participants were asked to perform isometric trapezoidal ramps consisting of a linear increase from 0% MVC to the target torque level in 5 seconds, a plateau phase at the target torque level for 30 seconds, and a linear decrease from the target torque level to 0% MVC in 5 seconds. Considering that contraction intensity can affect the neural drive to active motor units (Martinez-Valdes et al. 2022), hip extension and knee flexion isometric tasks were performed with two different intensities. Consequently, participants performed four isometric torque-matching tasks in total: knee flexion at 20% MVC, knee flexion at 40% MVC, hip extension at 20% MVC, hip extension at 40% MVC. The order of the tasks (knee flexion and hip extension) was randomized.

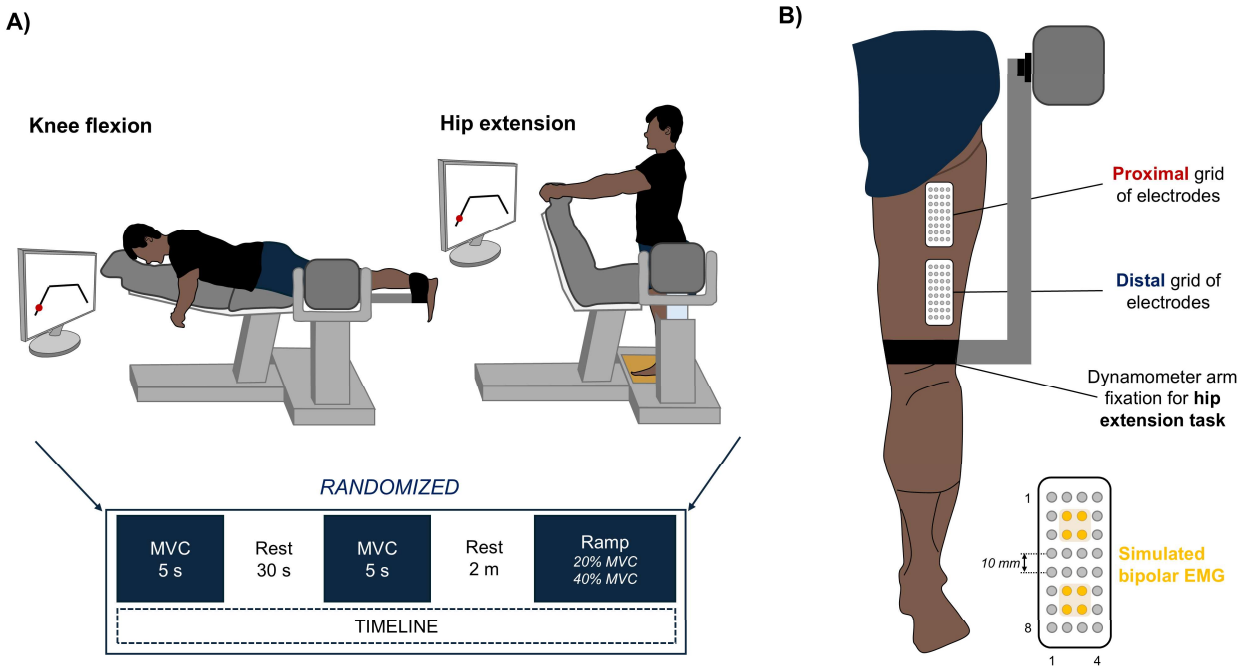

Figure 1: Experimental procedures. *(A) Participants performed isometric knee flexion and hip extension tasks. Two maximal voluntary contractions (MVCs) were conducted for each task followed by trapezoidal ramp contractions were at 20% and 40% of MVC (bottom part). (B) High-density surface electromyograms were recorded from the proximal and distal regions of the biceps femoris long head using grids of 32 electrode each. The yellow-highlighted electrodes indicate the specific channels used to simulate a bipolar sEMG configuration.*

Data collection

During the tasks, two semi-disposable 32-channel grids of electrodes (10 mm interelectrode distance, GR10MM0804, OTBioelettronica, Turin, Italy; bottom part of **Figure 1B**) were used to record the activity of the long head of the biceps femoris muscle. Before electrode placement, the skin was shaved and cleaned with neutral soap and water. With participants lying prone on a stretcher, the electrodes were positioned on the proximal and distal regions of the long head of the biceps femoris (**Figure 1B**). Ultrasound imaging (Logiq, GE Healthcare, USA) was used to identify and mark the aponeuroses of the biceps femoris muscle on the skin, ensuring precise grid placement. The grids were positioned as proximally and distally as possible on the muscle, aligned longitudinally with the fascicles, and not over adjacent muscles. The HDsEMG signals were recorded in monopolar mode and digitalized synchronously with the torque output at

a sampling frequency of 2000 Hz using a 16-bit wireless amplifier (10–500 Hz bandwidth; Gain 1; MUOVI, OTBioelettronica, Turin, Italy).

Data analysis

HDsEMG signals were analyzed offline using MATLAB (version 2022b, The MathWorks Inc., Natick, Massachusetts, USA) custom-written scripts. Monopolar EMGs were digitally filtered between 20 and 500 Hz using a second-order Butterworth band-pass filter. Each monopolar signal was visually inspected, and channels deemed unsuitable for analysis (e.g., containing artifacts) were excluded.

Bipolar sEMG amplitude. To compare proximodistal differences in the bipolar sEMG amplitude of the long head of the biceps femoris during knee flexion and hip extension tasks, we simulated two bipolar sEMG detection sites: one in the proximal region and one in the distal region. For each grid, we calculated the difference between the average monopolar signals from groups of four channels in a proximal and a distal location within the electrode grid (yellow channels indicated in the bottom part of **Figure 1B**). To quantify the biceps femoris muscle activation, the root-mean-square (RMS) amplitude was calculated in non-overlapping windows of 250 ms during the 30-s plateau phase, and the average RMS value across these windows was considered for further analysis. Additionally, we calculated the normalized RMS amplitude by dividing the average RMS value by the RMS amplitude during the MVC, which was computed as the RMS value in a 500-ms time window centered around the peak torque. The maximum MVC RMS value between proximal and distal bipolar sEMG was considered for the normalization.

182 *Motor unit decomposition*. HDsEMG signals from the proximal and distal grids were decomposed
183 separately into individual motor unit spike trains (**Figure 2A**) using a convolutive blind source
184 separation method (Negro et al. 2016). Briefly, after performing the convolutive sphering of the
185 HDsEMG signals (i.e., extending, centering, and whitening), a fixed-point algorithm was applied
186 to identify sources (i.e., motor unit spike trains) that maximize a measure of sparsity. Spikes were
187 separated from noise using K-means clustering, and as the motor unit separation vectors were
188 iteratively updated, the estimation of discharge times was further refined by minimizing the CoV
189 of the inter-spike intervals (for details, see Negro et al., 2016). Motor units automatically identified
190 by the algorithm were individually inspected and, when necessary, manually edited by an
191 experienced operator (Martinez-Valdes et al. 2023). The editing step is performed to improve the
192 accuracy of the identified motor unit discharge times, primarily by removing misidentified
193 discharges (e.g., inter-spike intervals < 20 ms) and adding missing dischargers (e.g., inter-spike
194 intervals > 250 ms). To ensure the analyzed motor units were exclusively from the proximal and
195 distal regions, duplicated motor units (i.e., those identified in both grids) were excluded from
196 further analysis. To this end, motor unit spike trains from the proximal and distal regions were
197 compared and considered to be generated by the same motor unit if they shared at least 30% of
198 discharge times (Negro et al. 2016).
199

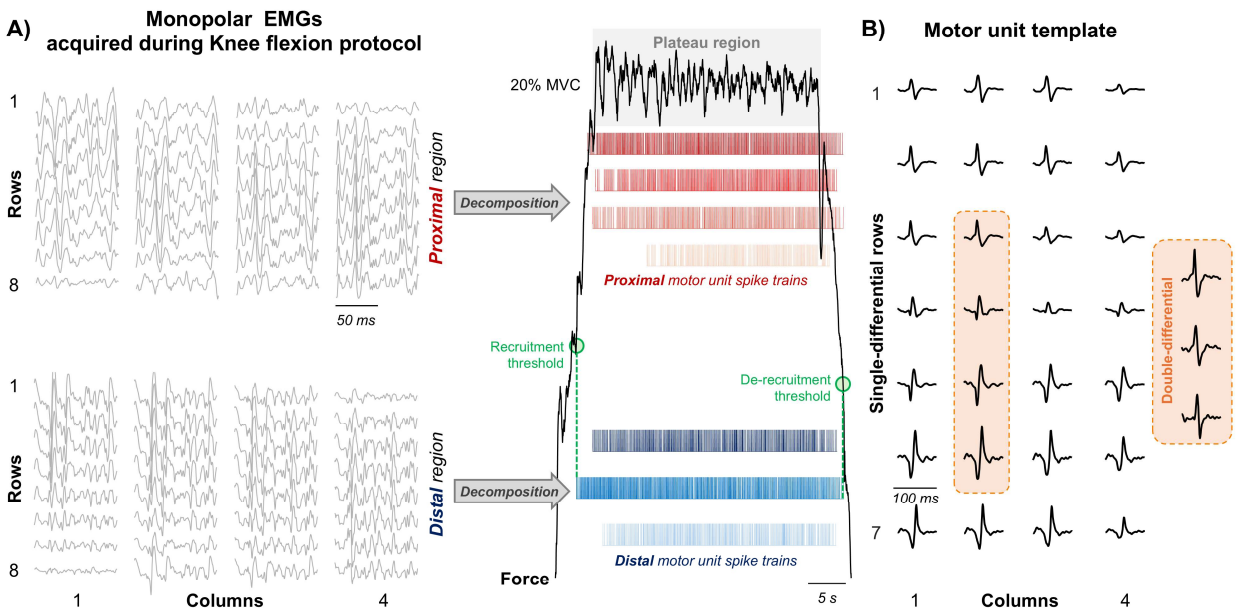

Figure 2: Calculation of motor unit properties. *(A) Monopolar surface electromyograms (sEMG) were decomposed into individual motor unit spike trains for each muscle region. Recruitment and de-recruitment thresholds were identified as the torque level (% maximal voluntary contraction) at which the motor unit first began and stop to discharge (green dashed lines), respectively. The mean discharge rate and discharge rate variability were calculated from the plateau phase (light grey rectangle) of the torque output (black line). (B) Motor unit action potential templates were obtained by triggering and averaging the single-differential sEMG within a 50 ms window centered on motor unit discharge times. The motor unit action potentials' peak-to-peak amplitudes were calculated from both the simulated bipolar sEMG detection sites and from the active channels of the grid. Motor unit conduction velocity was estimated using a multichannel maximum likelihood algorithm, selecting from three to six consecutive double-differential channels that displayed the clearest action potential propagation in each column of the grid (orange rectangle).*

<u>*Motor unit central properties*</u>. To quantify proximodistal differences in motor unit central properties of the long head of the biceps femoris muscle during knee flexion and hip extension tasks, the mean discharge rate, the discharge rate variability, the recruitment threshold, and the de-recruitment threshold were calculated for each motor unit. The instantaneous discharge rate of each motor unit was calculated from the multiplicative inverse of the inter-spike interval and the mean discharge rate during the plateau phase was considered for analysis. The motor unit discharge rate variability was computed as the CoV of the inter-spike interval (CoV-ISI). The motor unit recruitment threshold and de-recruitment threshold were determined by identifying the torque level

221 (%MVC) at which the motor unit first began and stop to discharge during the contraction,
222 respectively (green-dashed vertical lines in **Figure 2A**) (Gomes et al. 2024).
223
224 *Motor unit action potential properties*. To quantify proximodistal differences in motor unit action
225 potential (MUAP) properties of the long head of the biceps femoris muscle during knee flexion
226 and hip extension tasks, the MUAP amplitude and conduction velocity were calculated. MUAP
227 templates were estimated by triggering and averaging the single-differential sEMG signals at 50
228 ms windows centered at the discharge times of individual motor units (i.e., spike-triggered
229 averaging technique; Stein et al. 1972; **Figure 2B**). Two indices were used to assess MUAP
230 amplitude: (i) the peak-to-peak amplitude of the MUAP at the simulated bipolar sEMG detection
231 site (see *Bipolar sEMG amplitude* section), and (ii) the average peak-to-peak amplitude across the
232 MUAPs from the active channels of the grid. Active channels were defined as those with a peak-
233 to-peak amplitude greater than 70% of the maximum amplitude observed across the grid (Vieira
234 et al. 2010). The MUAP conduction velocity was measured from a minimum of three to a
235 maximum of six double-differential channels in each column of the grid using the multichannel
236 maximum likelihood algorithm (Farina et al. 2001). For each column, the channels that displayed
237 the clearest action potentials propagation were manually selected (see orange rectangle in **Figure**
238 **2B**), and the conduction velocity estimated from the column with the higher cross-correlation
239 across selected channels was considered for further analysis (Valli et al. 2024).
240
241 **Statistics**
242 Linear mixed-effect models (LMM) were applied to compare motor unit central properties
243 (mean discharge rate, CoV-ISI, recruitment threshold and de-recruitment threshold), motor unit
244 action potential properties (MUAP amplitude and MUAP conduction velocity), and bipolar sEMG

amplitude (raw and normalized) between the proximal and distal regions, and torque levels. For each task, random intercept models were used with region (proximal and distal) and torque level (20% and 40% MVC) as fixed effects and participant as random effect (*i.e., motor unit property or sEMG amplitude ~ 1 + region*torque + (1 | participant)*). These models were implemented using the package *lmerTest* (Kuznetsova et al. 2017) with the Kenward-Roger method to approximate the degrees of freedom and estimate the *P*-value. Q-Q plot inspection was used to assess the assumption of normality of residuals. The *emmeans* package was used, when necessary, for multiple comparisons and to determine estimated marginal means with 95% confidence intervals (Lenth et al. 2019). All statistical analyzes were conducted with the R programming language (version 4.2.0). All individual data are provided as supplementary material.

Results

Proximodistal differences in bipolar sEMG amplitude

To investigate proximodistal differences in the biceps femoris long head activation during knee flexion and hip extension tasks, we simulated two bipolar sEMG detection sites in each region and calculated the RMS amplitude value. For both the raw and normalized RMS values and for all investigated tasks, significantly greater bipolar sEMG amplitudes were detected at the distal region compared to the proximal region (LMM; $F > 9.87$; $P < 0.002$ for all cases), and at 40% MVC compared to 20% MVC (LMM; $F > 56.68$; $P < 0.001$ for all cases). Additionally, no significant interactions between torque level and region were observed (LMM; $F < 3.64$; $P > 0.06$ for all cases). At 20% MVC, the raw RMS amplitude values (mean ± SD) for knee flexion were 42.9 ± 26.9 μV in the proximal region and 74.9 ± 37.8 μV in the distal region. For hip extension, the values were 58.1 ± 34.9 μV in the proximal region and 90.8 ± 72.9 μV in the distal region. At 40% MVC, knee flexion showed 139 ± 58.3 μV in the proximal region and 201 ± 55.5 μV in the distal

region, while hip extension showed 131 ± 67.9 µV in the proximal region and 166 ± 84.7 µV in the distal region. Normalized bipolar RMS amplitude results are presented in **Figure 3**.

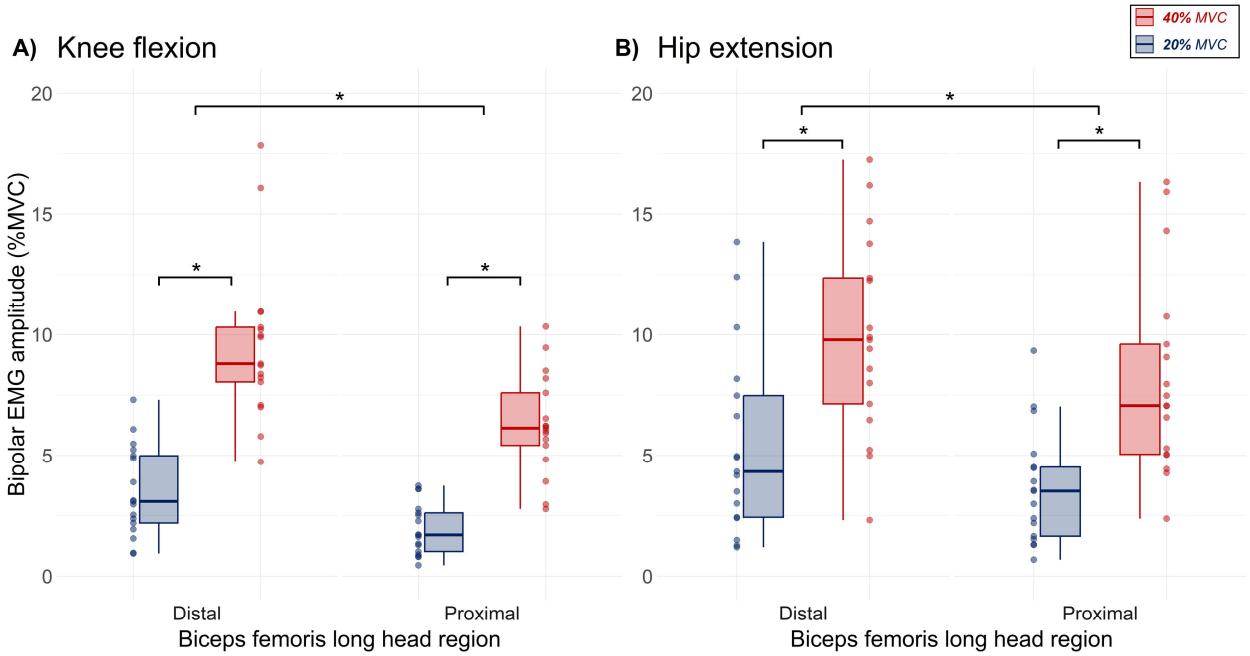

Figure 3: Bipolar EMG amplitude results. *Normalized root-mean-square amplitude values from simulated bipolar sEMG at 20% of maximal voluntary contraction (MVC) (blue) and 40% MVC (red), separately for knee flexion (A) and hip extension (B) tasks. Horizontal traces, boxes, and whiskers, respectively, denote median value, interquartile interval, and distribution range. Asterisk denotes statistical differences between distal and proximal muscle regions (P < 0.05).*

Proximodistal differences in motor unit central properties

To assess whether there were proximodistal differences in motor unit central properties of the biceps femoris long head during knee flexion and hip extension tasks, we compared the mean discharge rate, discharge rate variability (CoV-ISI), recruitment threshold and de-recruitment threshold of decomposed motor units. When pooling motor units from the proximal and distal regions, an average of 6 ± 4 and 5 ± 4 motor units were identified per participant for the knee flexion at 20% MVC and knee flexion at 40% MVC, respectively. For hip extension tasks, 6 ± 5

and 3 ± 3 motor units were identified per participant for the hip extension at 20% MVC and hip extension at 40% MVC, respectively.

For all the tasks, no significant differences in motor unit mean discharge rate were observed between the proximal and distal regions of the biceps femoris long head (LMM; F < 1.20; P > 0.274 for all cases; **Figure 4**). Conversely, significant increases in mean discharge rate of approximately 1.8 pps and 4.1 pps were observed between 20% and 40% MVC for knee flexion (**Figure 4A**) and hip extension (**Figure 4B**), respectively (LMM; F > 14.37; P < 0.001 for all cases).

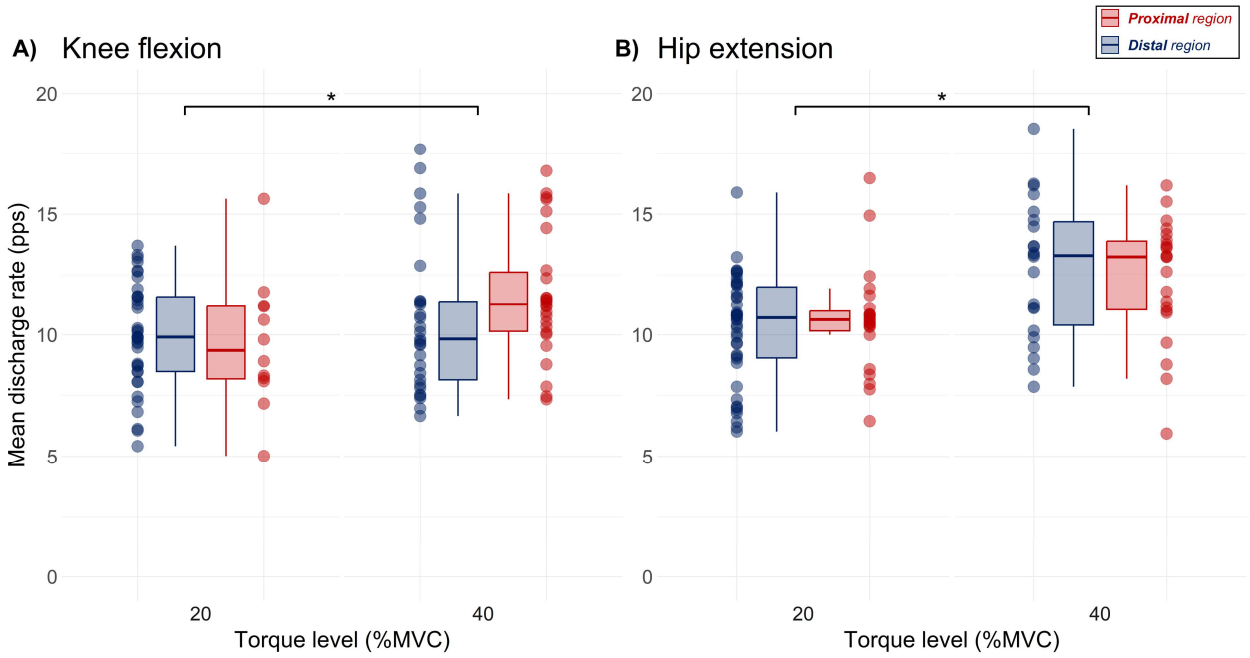

Figure 4: Mean discharge rate results. *Mean discharge rate values of motor units decomposed from the proximal (red) and distal (blue) regions of the biceps femoris long head, separately for knee flexion (A) and hip extension (B) tasks. Data is grouped by torque level. Horizontal traces, boxes, and whiskers, respectively, denote median value, interquartile interval, and distribution range. Asterisk denotes statistical differences between 20% and 40% of maximal voluntary contraction (MVC) (P < 0.05).*

Regarding motor unit discharge rate variability, significant increases of ~3% in CoV-ISI were observed between 20% and 40% MVC only for the knee flexion task (LMM; F = 6.65; P =

0.012). No significant differences were observed across torque levels (LMM; F = 0.975; $P = 0.326$) and between the proximal and distal regions of the biceps femoris long head for the hip extension task (LMM; F = 2.23; $P = 0.634$). At 20% MVC, the CoV-ISI values (mean ± SD) for knee flexion were 16.5 ± 4.21% in the distal region and 15.9 ± 4.53% in the proximal region, while for hip extension the values were 19.3 ± 6.00% and 21.6 ± 7.80% in the distal and proximal regions respectively. At 40% MVC, knee flexion showed 22.2 ± 7.18% in the distal region and 19.8 ± 6.11% in the proximal, while hip extension showed 21.7 ± 6.20% and 21.0 ± 5.79% in the distal and proximal regions, respectively.

For both tasks, significant increases in the motor unit recruitment threshold (LMM; F > 133.56; $P < 0.001$ for all cases; **Online Resource 1**) and de-recruitment threshold (LMM; F > 244.89; $P < 0.001$ for all cases; **Online Resource 2**) were found between 20% and 40% of MVC. Conversely, no significant differences in recruitment and de-recruitment thresholds were observed between the proximal and distal regions (LMM; F < 2.058; $P > 0.119$ for all cases).

Proximodistal differences in motor unit action potential properties

To evaluate proximodistal differences in MUAP properties, we calculated the MUAP amplitude as (i) the peak-to-peak amplitude of MUAP at the simulated bipolar sEMG site, and (ii) the average peak-to-peak amplitude across the MUAPs from the active channels of the grid. For the knee flexion and hip extension tasks and both MUAP amplitude indexes, significant great amplitudes were observed for the distal region of the biceps femoris long head (LMM; F > 4.04; $P > 0.049$ for all cases), except for the MUAP at the simulated bipolar sEMG during the knee flexion task (LMM; F = 3.54, P = 0.064). Additionally, significant increases in both MUAP amplitude indexes were observed between 20% and 40% MVC (LMM; F > 7.42; $P < 0.008$ for all cases). The MUAP amplitude from active channels are presented in **Figure 5**.

We also quantified MUAP conduction velocity to assess proximodistal differences in MUAP properties. For both knee flexion (**Figure 5A**) and hip extension (**Figure 5B**) tasks, significantly higher MUAP conduction velocities were observed in the distal region compared to the proximal region (LMM; F > 4.45; $P < 0.038$ for all cases). Additionally, no significant main effect of torque level or interactions between torque level and region were observed (LMM; F < 1.39; $P > 0.241$ for all cases).

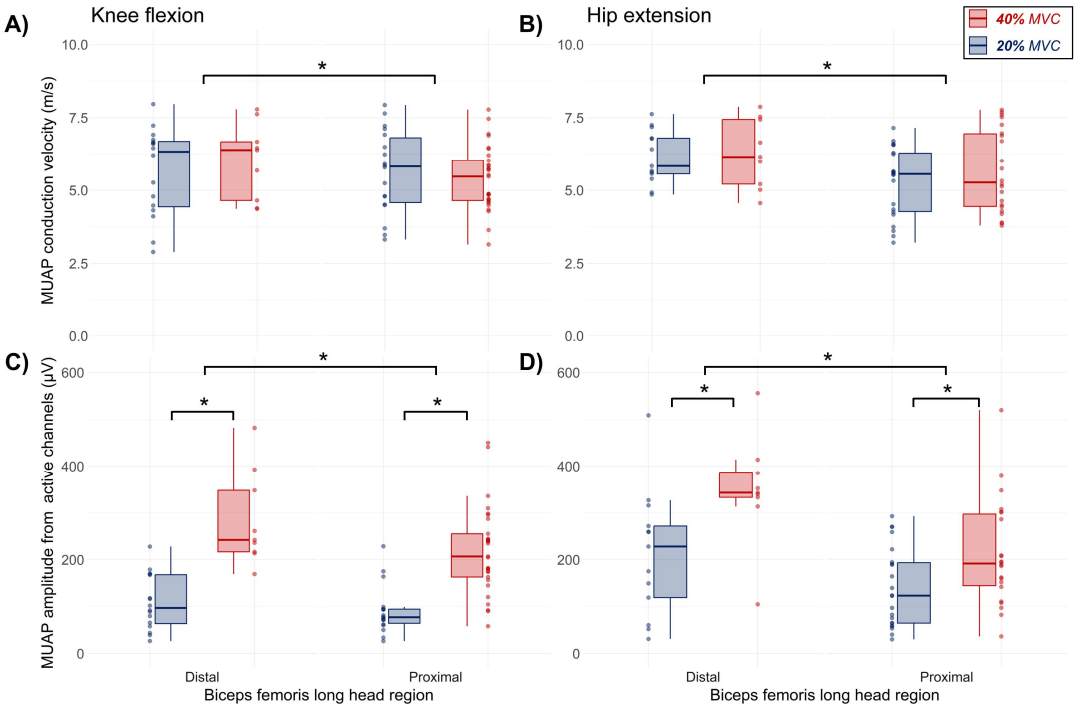

Figure 5: Motor unit action potential amplitude and conduction velocity results. *Motor unit action potential amplitude from active channels and motor unit conduction velocity results of motor units decomposed at 20% of maximal voluntary contraction (MVC) (blue) and 40% MVC (red), separately for knee flexion (A and C) and hip extension (B and D) tasks. Horizontal traces, boxes, and whiskers, respectively, denote median value, interquartile interval, and distribution range. Asterisk denotes statistical differences between distal and proximal muscle regions (P < 0.05).*

Discussion

The present study investigated proximodistal differences in the activity of the biceps femoris long head during isometric hip extension and knee flexion tasks. Our primary findings

346 demonstrated consistently greater bipolar sEMG amplitudes at the distal region compared to the
347 proximal region, regardless of the task performed. Additionally, while no significant differences
348 were observed in the motor unit central properties, the distal region showed significantly higher
349 MUAP conduction velocities and MUAP amplitudes than the proximal region. As discussed
350 below, these results suggest that the increased activation in the distal region of the biceps femoris
351 long head during both knee flexion and hip extension tasks is not related to differences in neural
352 control of motor units between regions, but it is likely attributed to the size and characteristics of
353 the motor unit action potentials.
354
355 ***Proximodistal activation within the biceps femoris long head during knee flexion and hip***
356 ***extension tasks***
357 Regional activation within human skeletal muscles has been consistently demonstrated
358 during voluntary contractions, particularly in muscles that contribute to multiple joint actions
359 (Staudenmann et al. 2009; Watanabe et al. 2012; de Souza et al. 2017; Cabral et al. 2022; Albarello
360 et al. 2022). This non-uniform activation requires a specific neuroanatomical organization,
361 wherein multiple branches of the nerve innervate localized regions within the muscle (i.e., motor
362 unit with relatively small territories; Watanabe et al., 2021). Such patterns have been previously
363 observed in the gastrocnemius (Segal et al. 1991) and rectus femoris (Yang and Morris 1999).
364 Notably, the biceps femoris muscle is innervated by two branches of the sciatic nerve, which insert
365 at multiple locations along its proximodistal axes (Seidel et al. 1996). Given this innervation
366 pattern, it is reasonable to hypothesize region-specific activation within this muscle.
367 Consistent with this hypothesis, our study reported localized activation of the biceps
368 femoris long head during both knee flexion and hip extension tasks, with the distal region
369 exhibiting consistently higher bipolar sEMG amplitude compared to the proximal region (**Figure**

370 **3**). These results align with previous studies that reported greater sEMG amplitudes in the distal
371 region during knee flexion tasks (Schoenfeld et al. 2015; Hegyi et al. 2018, 2019; Miyamoto and
372 Hirata 2021). However, in contrast to our findings, previous evidence has suggested a more
373 homogeneous proximodistal activation pattern within the biceps femoris during hip extension tasks
374 (Schoenfeld et al. 2015; Hegyi et al. 2018). These discrepancies may be attributable to
375 methodological differences, particularly in contraction type and task specificity. Our study used
376 isometric tasks without torque at the knee joint (the tested limb was slightly suspended, and the
377 dynamometer arm was fixed above the popliteal fossa; see **Figure 1B)**, which may differ from the
378 activation patterns in dynamic conditions. Additionally, methodological factors must be
379 considered when interpreting sEMG amplitude as an indicator of neural drive to the muscle.

380 Ideally, the sEMG signal reflects the strength of the neural drive to the muscle and its
381 amplitude properties have traditionally been used to infer neural control strategies (Del Vecchio
382 et al. 2017). However, sEMG amplitude is also influenced by the amplitude and duration of the
383 MUAPs (see equation 2 in Farina et al. 2014). Additionally, the estimation of sEMG amplitude is
384 always lower than the sum of individual MUAP amplitudes due to a phenomenon known as
385 amplitude cancellation (Day and Hulliger 2001; Keenan et al. 2005; Negro et al. 2015). In addition,
386 factors such as muscle fiber properties (e.g., MUAP size and conduction velocity) (Farina et al.
387 2014; Del Vecchio et al. 2017), muscle architecture (Vieira et al. 2017), and inter-electrode
388 distance and placement (Vieira et al. 2023) have been shown to directly affect sEMG amplitude.
389 Therefore, the higher activation in the distal region of the biceps femoris long head during knee
390 flexion cannot be necessarily inferred as an increased neural drive to this region compared to the
391 proximal region, as differences in sEMG amplitudes between anatomical locations may also be
392 influenced by MUAP amplitude (Martinez-Valdes et al. 2018). To better address this issue, we
393 decomposed HDsEMG signals to analyze individual motor unit activity, allowing us to examine

394 both central and action potential properties and provide more accurate insights into the
395 mechanisms underlying the observed activation differences.
396
397 ***Motor unit action potential properties, not discharge rate modulation, explain localized***
398 ***activation in the biceps femoris long head***
399 A possible explanation for the regional activation within a muscle is the differential
400 modulation of presynaptic inputs to alpha motor neurons that innervate specific regions (Watanabe
401 et al. 2021), as suggested in muscles such as the first dorsal interosseous during flexion and
402 abduction tasks (Desmedt & Godaux 1981) and the rectus femoris during cutaneous electrical
403 stimulation (Watanabe et al. 2015). The most reliable method to investigate this possibility is
404 through the assessment of individual motor unit central properties (mean discharge rate, discharge
405 rate variability and CoV-ISI) as well as time- and frequency-domain coupling between motor unit
406 discharge patterns, as conducted in several recent studies (Cabral et al. 2018; Cabral et al., 2024;
407 Cohen et al. 2020; Sahinis et al. 2024; Crouzier et al. 2024). Regarding the hamstrings, recently,
408 Sahinis et al. (2024) observed distinct neural drive along the semitendinosus muscle during
409 isometric knee flexion tasks. Specifically, the mean discharge rate was greater for motor units in
410 the proximal region compared to the distal region. Moreover, neural drive variability was higher
411 in the proximal at the three lower target forces (10%, 20%, and 40%) and across all three knee
412 joint angles (0°: long length, 45°: intermediate length, and 90°: short length). These findings
413 suggest region-specific motor unit discharge characteristics and neural control in the
414 semitendinosus across varying muscle lengths.
415 In contrast, our study did not observe any difference in mean discharge rate (**Figure 4**),
416 CoV-ISI values, or recruitment and de-recruitment thresholds (**Online Resources 1 and 2**)
417 between the proximal and distal regions of the biceps femoris long head. These results indicate

418 that, unlike the semitendinosus, motor units located in different proximodistal regions of the biceps
419 femoris long head are modulated similarly during isometric tasks. Given that both of these
420 hamstring muscles are biarticular and share similar functions (Kellis and Blazevich 2022), it is
421 intriguing that motor units in the semitendinosus exhibit region-specific neural drive during knee
422 flexion, while those in the biceps femoris long head do not. There are several potential explanations
423 for these differences. Although both muscles are innervated proximodistally by different branches
424 of the sciatic nerve (Seidel et al. 1996), the semitendinosus has two distinct proximodistal regions
425 separated by a tendinous inscription, with each region innervated by a separate nerve branch (see
426 Figure 2 in Woodley & Mercer, 2005). This specific neuroanatomical organization may facilitate
427 region-specific motor unit modulation in this muscle, as observed by Sahinis et al. (2024).
428 Additionally, the presence of the biceps femoris short head may contribute to the differences
429 between semitendinosus and biceps femoris long head. For instance, the short head is innervated
430 separately from the long head by a single nerve branch originating from the common fibular nerve
431 (Farfán et al. 2024). This distinct innervation arrangement could influence the modulation of neural
432 drive along the long head, potentially resulting in less pronounced proximodistal motor unit
433 activity during both knee flexion and hip extension tasks. Although these potential explanations
434 provide insight into the observed differences, further research is required to explore motor unit
435 discharge properties across different regions of both the semitendinosus and biceps femoris long
436 head, ideally through simultaneous recordings.

437 To investigate whether potential proximodistal differences in the MUAP properties of
438 biceps femoris long head motor units could explain the observed differences in sEMG amplitude,
439 we calculated MUAP amplitude and MUAP conduction velocity, which are two commonly used
440 parameters in the literature (Martinez-Valdes et al. 2018; Valli et al. 2024). Consistent with the
441 sEMG amplitude results, higher MUAP amplitudes and conduction velocities were observed in

442 the distal region of the biceps femoris long head compared to the proximal region. Changes in
443 these motor unit action potential properties, rather than central properties, have previously been
444 associated with changes in sEMG amplitude (Martinez-Valdes et al. 2018). Collectively, these
445 findings suggest that the greater sEMG amplitudes observed in the biceps femoris long head during
446 knee flexion and hip extension tasks are primarily driven by action potential properties, rather than
447 discharge statistics.

448 The localized differences in motor unit action potential properties, and consequently
449 bipolar sEMG amplitude, in the biceps femoris long head are likely explained by anatomical and
450 mechanical differences within the muscle. Miyamoto & Hirata (2021) recently reported that during
451 isometric knee flexion at 20% of MVC, the distal region of the biceps femoris long head exhibited
452 greater stiffness, as measured by supersonic shear wave elastography, compared to the central and
453 proximal regions. The authors also observed higher sEMG amplitudes in the distal region, which
454 aligns with both the current study and previous findings (Schoenfeld et al. 2015; Hegyi et al. 2018,
455 2019). This increased stiffness in the distal region may result from architectural variations within
456 the muscle, as the biceps femoris long head has longer fibers and a greater pennation angle
457 proximally, which could lead to reduced strain in the proximal region (Kellis 2018). While this
458 relationship between localized peripheral motor unit activity, sEMG amplitude and the muscle's
459 architecture appears plausible, further investigation is required to fully understand these
460 mechanisms.

461

462 **Methodological considerations and limitations**

463 When assessing muscle activation using conventional bipolar electromyography, several
464 critical factors must be considered such as the location of the innervation zone (Mancebo et al.
465 2019), the direction of the task (Lulic-Kuryllo et al. 2022), and the selection of representative sites

466 within muscle regions (Cabral et al. 2022; Albarello et al. 2022). Our results highlight such
467 considerations, suggesting that bipolar sEMG amplitudes obtained from a single region of the
468 biceps femoris may not accurately represent global muscle activity during knee flexion and hip
469 extension tasks, likely due to peripheral factors.

470 However, some limitations of our study should be acknowledged. First, the relatively low
471 number of motor units identified in each region may limit the generalizability of our findings.
472 Future research should aim to address this by incorporating larger and denser surface grids of
473 electrodes, which could potentially capture a greater number of motor units (Caillet et al. 2023).
474 Second, we assessed the biceps femoris long head at a single muscle length during both knee
475 flexion and hip extension tasks. Considering recent evidence suggesting that changes in muscle
476 length directly influence the shared synaptic oscillations to spinal motor neurons (Cabral et al.
477 2024), it would be interesting to investigate whether similar responses occur when altering knee
478 and hip joint angles. Additionally, while the proximal grid of electrodes was positioned as close
479 as possible to the origin of the biceps femoris (see *Methods*), the superficial nature of the gluteus
480 muscle compromised optimal placement. In this regard, techniques such as functional magnetic
481 resonance imaging could enhance precision in analyzing the proximal region of the biceps femoris
482 (Schuermans et al. 2014). Lastly, due to the limited number of probes available, the activity of
483 other hamstring muscles was not explored in this study, which represents another avenue for future
484 research.

485

486 **Conclusions**

487 Considering that the long head of the biceps femoris shows the highest prevalence of
488 injuries among the hamstrings, with injuries occurring in the proximal, central, and distal regions
489 of this muscle (Grange et al. 2023), this study provides interesting insights into the proximodistal

differences in biceps femoris long head activity during isometric knee flexion and hip extension tasks. Our findings indicate that greater sEMG amplitude in the distal region of the biceps femoris long head cannot be attributed to differences in neural drive between proximal and distal regions, as no significant variations were observed in central motor unit properties. Instead, the increased distal activation appears to be driven by motor unit action potential properties, likely influenced by intra-muscular anatomic and mechanical variations. Furthermore, this study emphasizes the limitations of relying solely on sEMG amplitude to infer neural control strategies across different regions of the biceps femoris long head.

Authors' Contributions

All the authors contributed substantially to the manuscript. Conception and design of the experiments (JCSA, HVC, LFO), collection of data (JCSA), analysis of data (JCSA, HVC, FN), interpretation of data (JCSA, HVC, FN, LFO), drafting the article and revising it critically for important intellectual content (JCSA, HVC, FN, LFO), and final approval of the version to be published (JCSA, HVC, FN, LFO). All authors have read and approved the final version of the manuscript and agree with the order of presentation of the authors.

Competing interests

The authors declare that they have no competing interests.

References

Afonso J, Rocha-Rodrigues S, Clemente FM, et al (2021) The Hamstrings: Anatomic and Physiologic Variations and Their Potential Relationships With Injury Risk. Front Physiol 12

Albarello JC dos S, Cabral H V., Leitão BFM, et al (2022) Non-uniform excitation of pectoralis major induced by changes in bench press inclination leads to uneven variations in the cross-sectional area measured by panoramic ultrasonography. Journal of Electromyography and Kinesiology 67:102722. https://doi.org/10.1016/j.jelekin.2022.102722

Brukner P (2015) Hamstring injuries: Prevention and treatment - An update. Br J Sports Med 49:1241–1244. https://doi.org/10.1136/bjsports-2014-094427

Cabral H V., de Souza LML, de Oliveira LF, Vieira TM (2022) Non-uniform excitation of the pectoralis major muscle during flat and inclined bench press exercises. Scand J Med Sci Sports 32:381–390. https://doi.org/10.1111/sms.14082

Cabral H V., de Souza LML, Mello RGT, et al (2018) Is the firing rate of motor units in different vastus medialis regions modulated similarly during isometric contractions? Muscle Nerve 57:279–286. https://doi.org/10.1002/mus.25688

Cabral H V., Inglis JG, Cudicio A, et al (2024) Muscle contractile properties directly influence shared synaptic inputs to spinal motor neurons. J Physiol 602:2855–2872. https://doi.org/10.1113/JP286078

Caillet AH, Avrillon S, Kundu A, et al (2023) Larger and Denser: An Optimal Design for Surface Grids of EMG Electrodes to Identify Greater and More Representative Samples of Motor Units. eNeuro 10:. https://doi.org/10.1523/ENEURO.0064-23.2023

Cohen JW, Gallina A, Ivanova TD, et al (2020) Regional modulation of the ankle plantarflexor muscles associated with standing external perturbations across different directions. Exp Brain Res 238:39–50. https://doi.org/10.1007/s00221-019-05696-8

Crouzier M, Avrillon S, Hug F, Cattagni T (2024) Horizontal foot orientation affects the distribution of neural drive between gastrocnemii during plantarflexion, without changing neural excitability. J Appl Physiol. https://doi.org/10.1152/japplphysiol.00536.2023

Danielsson A, Horvath A, Senorski C, et al (2020) The mechanism of hamstring injuries- A systematic review. BMC Musculoskelet Disord 21

Day SJ, Hulliger M (2001) Experimental Simulation of Cat Electromyogram: Evidence for Algebraic Summation of Motor-Unit Action-Potential Trains. J Neurophysiol 86:2144–2158. https://doi.org/10.1152/jn.2001.86.5.2144

de Souza LML, da Fonseca DB, Cabral H da V, et al (2017) Is myoelectric activity distributed equally within the rectus femoris muscle during loaded, squat exercises? Journal of Electromyography and Kinesiology 33:10–19. https://doi.org/10.1016/j.jelekin.2017.01.003

Desnedt JE, Gidaux E (1981) Spinal Motoneuron Recruitment in Man: Rank Deordering with Direction But Not with Speed of Voluntary Movement. Science (1979) 214:933–936. https://doi.org/10.1126/science.7302570

Ekstrand J, Bengtsson H, Waldén M, et al (2023) Hamstring injury rates have increased during recent seasons and now constitute 24% of all injuries in men's professional football: the UEFA Elite Club Injury Study from 2001/02 to 2021/22. Br J Sports Med 57:292–298. https://doi.org/10.1136/bjsports-2021-105407

Farfán E, Rojas S, Olivé-Vilás R, Rodríguez-Baeza A (2024) Innervation patterns of hamstring muscles, including morphological descriptions and clinical implication. Surgical and Radiologic Anatomy 46:749–760. https://doi.org/10.1007/s00276-024-03371-4

Farina D, Holobar A, Merletti R, Enoka RM (2010) Decoding the neural drive to muscles from the surface electromyogram. Clinical Neurophysiology 121:1616–1623

Farina D, Merletti R, Enoka RM (2004) Downloaded from journals.physiology.org/journal/jappl. J Appl Physiol 96:1486–1495. https://doi.org/10.1152/japplphysiol.01070.2003.-This

Farina D, Merletti R, Enoka RM (2014) The extraction of neural strategies from the surface EMG: An update. J Appl Physiol 117:1215–1230. https://doi.org/10.1152/japplphysiol.00162.2014

Farina D, Muhammad W, Fortunato E, et al (2001) Estimation of single motor unit conduction velocity from surface electromyogram signals detected with linear electrode arrays

Fields KB, Bloom OJ, Priebe D, Foreman B (2005) Basic biomechanics of the lower extremity. Primary Care - Clinics in Office Practice 32:245–251

Gomes MM, Jenz ST, Beauchamp JA, et al (2024) Voluntary co-contraction of ankle muscles alters motor unit discharge characteristics and reduces estimates of persistent inward currents. J Physiol 602:4237–4250. https://doi.org/10.1113/JP286539

Grange S, Reurink G, Nguyen AQ, et al (2023) Location of Hamstring Injuries Based on Magnetic Resonance Imaging: A Systematic Review. Sports Health 15:111–123

Hegyi A, Csala D, Péter A, et al (2019) High-density electromyography activity in various hamstring exercises. Scand J Med Sci Sports 29:34–43. https://doi.org/10.1111/sms.13303

Hegyi A, Péter A, Finni T, Cronin NJ (2018) Region-dependent hamstrings activity in Nordic hamstring exercise and stiff-leg deadlift defined with high-density electromyography. Scand J Med Sci Sports 28:992–1000. https://doi.org/10.1111/sms.13016

Hogervorst T, Vereecke EE (2015) Evolution of the human hip. Part 2: muscling the double extension. J Hip Preserv Surg 2:3–14. https://doi.org/10.1093/jhps/hnu014

Holobar A, Zazula D (2007) Multichannel Blind Source Separation Using Convolution Kernel Compensation. IEEE Transactions on Signal Processing 55:4487–4496. https://doi.org/10.1109/TSP.2007.896108

Jokela A, Valle X, Kosola J, et al (2023) Mechanisms of Hamstring Injury in Professional Soccer Players: Video Analysis and Magnetic Resonance Imaging Findings. Clinical Journal of Sport Medicine 33:217–224. https://doi.org/10.1097/JSM.0000000000001109

Jonhagen S, Meth N;, Eriksson E, J6nhagen S Hamstring Injuries in Sprinters The Role of Concentric and Eccentric Hamstring Muscle Strength and Flexibility

Keenan KG, Farina D, Maluf KS, et al (2005) Influence of amplitude cancellation on the simulated surface electromyogram. J Appl Physiol 98:120–131. https://doi.org/10.1152/japplphysiol.00894.2004

Kellis E (2018) Intra- and Inter-Muscular Variations in Hamstring Architecture and Mechanics and Their Implications for Injury: A Narrative Review. Sports Medicine 48:2271–2283

Kellis E, Blazevich AJ (2022) Hamstrings force-length relationships and their implications for angle-specific joint torques: a narrative review. BMC Sports Sci Med Rehabil 14:166. https://doi.org/10.1186/s13102-022-00555-6

Kuznetsova A, Brockhoff PB, Christensen RHB (2017) lmerTest Package: Tests in Linear Mixed Effects Models. J Stat Softw 82:1–26. https://doi.org/10.18637/JSS.V082.I13

LENTH R, SINGMANN H, LOVE J, et al (2019) Package ‘emmeans’.

Liu H, Garrett WE, Moorman CT, Yu B (2012) Injury rate, mechanism, and risk factors of hamstring strain injuries in sports: A review of the literature. J Sport Health Sci 1:92–101

Lulic-Kuryllo T, Negro F, Jiang N, Dickerson CR (2022) Differential regional pectoralis major activation indicates functional diversity in healthy females. J Biomech 133:. https://doi.org/10.1016/j.jbiomech.2022.110966

Mancebo FD, Cabral H V., de Souza LML, et al (2019) Innervation zone locations distribute medially within the pectoralis major muscle during bench press exercise. Journal of Electromyography and Kinesiology 46:8–13. https://doi.org/10.1016/j.jelekin.2019.03.002

Maniar N, Carmichael DS, Hickey JT, et al (2022) Incidence and prevalence of hamstring injuries in field-based team sports: A systematic review and meta-analysis of 5952 injuries from over 7 million exposure hours. Br J Sports Med 57:109–116

Martinez-Valdes E, Enoka RM, Holobar A, et al (2023) Consensus for experimental design in electromyography (CEDE) project: Single motor unit matrix. Journal of Electromyography and Kinesiology 68:. https://doi.org/10.1016/j.jelekin.2022.102726

Martinez-Valdes E, Negro F, Botter A, et al (2022) Modulations in motor unit discharge are related to changes in fascicle length during isometric contractions. J Appl Physiol 133:1136–1148. https://doi.org/10.1152/japplphysiol.00758.2021

Martinez-Valdes E, Negro F, Falla D, et al (2018) Surface electromyographic amplitude does not identify differences in neural drive to synergistic muscles. J Appl Physiol 124:1071–1079. https://doi.org/10.1152/japplphysiol.01115.2017.-Surface

Miyamoto N, Hirata K (2021) Site-specific features of active muscle stiffness and proximal aponeurosis strain in biceps femoris long head. Scand J Med Sci Sports 31:1666–1673. https://doi.org/10.1111/sms.13973

Miyamoto N, Wakahara T, Kawakami Y (2012) Task-dependent inhomogeneous muscle activities within the Bi-articular human rectus femoris muscle. PLoS One 7:. https://doi.org/10.1371/journal.pone.0034269

Negro F, Keenan K, Farina D (2015) Power spectrum of the rectified EMG: when and why is rectification beneficial for identifying neural connectivity? J Neural Eng 12:036008. https://doi.org/10.1088/1741-2560/12/3/036008

Negro F, Muceli S, Castronovo AM, et al (2016) Multi-channel intramuscular and surface EMG decomposition by convolutive blind source separation. J Neural Eng 13:026027. https://doi.org/10.1088/1741-2560/13/2/026027

Opar DA, Williams MD, Shield AJ Hamstring Strain Injuries Factors that Lead to Injury and Re-Injury

Ribeiro-Alvares JB, Dornelles MP, Fritsch CG, et al (2020) Prevalence of hamstring strain injury risk factors in professional and under-20 male football (Soccer) players. J Sport Rehabil 29:339–345. https://doi.org/10.1123/jsr.2018-0084

Sahinis C, Amiridis IG, Kannas T, et al (2024) Distinct Neural Drives along the Semitendinosus Muscle. Med Sci Sports Exerc. https://doi.org/10.1249/MSS.0000000000003530

Schoenfeld BJ, Contreras B, Tiryaki-Sonmez G, et al (2015) Regional Differences in Muscle Activation During Hamstrings Exercise. J Strength Cond Res 29:159–164. https://doi.org/10.1519/JSC.0000000000000598

Schuermans J, Van Tiggelen D, Danneels L, Witvrouw E (2014) Biceps femoris and semitendinosus - Teammates or competitors? New insights into hamstring injury mechanisms in male football players: A muscle functional MRI study. Br J Sports Med 48:1599–1606. https://doi.org/10.1136/bjsports-2014-094017

Segal RL, Wolf SL, DeCamp MJ, et al (1991) Anatomical Partitioning of Three Multiarticular Human Muscles. Cells Tissues Organs 142:261–266. https://doi.org/10.1159/000147199

Seidel PMP, Seidel GK, Gans BM, Dijkers M (1996) Precise localization of the motor nerve branches to the hamstring muscles: An aid to the conduct of neurolytic procedures. Arch Phys Med Rehabil 77:1157–1160. https://doi.org/10.1016/S0003-9993(96)90140-9

Staudenmann D, Kingma I, Daffertshofer A, et al (2009) Heterogeneity of muscle activation in relation to force direction: A multi-channel surface electromyography study on the triceps surae muscle. Journal of Electromyography and Kinesiology 19:882–895. https://doi.org/10.1016/j.jelekin.2008.04.013

Stein RB, French AS, Mannard A, Yemm R (1972) New methods for analysing motor function in man and animals. Brain Res 40:187–192. https://doi.org/10.1016/0006-8993(72)90126-6

Valli G, Ritsche P, Casolo A, et al (2024) Tutorial: Analysis of central and peripheral motor unit properties from decomposed High-Density surface EMG signals with openhdemg. Journal of Electromyography and Kinesiology 74:102850. https://doi.org/10.1016/j.jelekin.2023.102850

Vecchio A Del, Negro F, Felici F, Farina D (2017) Associations between motor unit action potential parameters and surface EMG features. J Appl Physiol 123:835–843. https://doi.org/10.1152/japplphysiol.00482.2017.-The

Vieira TM, Bisi MC, Stagni R, Botter A (2017) Changes in tibialis anterior architecture affect the amplitude of surface electromyograms. J Neuroeng Rehabil 14:. https://doi.org/10.1186/s12984-017-0291-5

Vieira TM, Cerone GL, Botter A, et al (2023) The Sensitivity of Bipolar Electromyograms to Muscle Excitation Scales With the Inter-Electrode Distance. IEEE Transactions on Neural Systems and Rehabilitation Engineering 31:4245–4255. https://doi.org/10.1109/TNSRE.2023.3325132

Vieira TMM, Merletti R, Mesin L (2010) Automatic segmentation of surface EMG images: Improving the estimation of neuromuscular activity. J Biomech 43:2149–2158. https://doi.org/10.1016/j.jbiomech.2010.03.049

Watanabe K, Kouzaki M, Ando R, et al (2015) Non-uniform recruitment along human rectus femoris muscle during transcutaneous electrical nerve stimulation. Eur J Appl Physiol 115:2159–2165. https://doi.org/10.1007/s00421-015-3196-7

Watanabe K, Kouzaki M, Moritani T (2016) Effect of electrode location on task-dependent electromyography responses within the human biceps femoris muscle. J Appl Biomech 32:97–100. https://doi.org/10.1123/jab.2015-0017

Watanabe K, Kouzaki M, Moritani T (2012) Task-dependent spatial distribution of neural activation pattern in human rectus femoris muscle. Journal of Electromyography and Kinesiology 22:251–258. https://doi.org/10.1016/j.jelekin.2011.11.004

Watanabe K, Vieira TM, Gallina A, et al (2021) Novel Insights Into Biarticular Muscle Actions Gained From High-Density Electromyogram. Exerc Sport Sci Rev 49:179–187. https://doi.org/10.1249/JES.0000000000000254

Wolf SL, Segal RL, English AW (1993) Task-oriented EMG activity recorded from partitions in human lateral gastrocnemius muscle. Journal of Electromyography and Kinesiology 3:87–94. https://doi.org/10.1016/1050-6411(93)90003-F

Woodley SJ, Mercer SR (2005) Hamstring muscles: Architecture and innervation. Cells Tissues Organs 179:125–141. https://doi.org/10.1159/000085004

Yang D, Morris SF (1999) Neurovascular anatomy of the rectus femoris muscle related to functioning muscle transfer. Plast Reconstr Surg 104:102–6

Zachazewski J, Silvers H, Li B, et al (2019) PREVALENCE OF HAMSTRING INJURIES IN SUMMER LEAGUE BASEBALL PLAYERS. Int J Sports Phys Ther 14:885–897. https://doi.org/10.26603/ijspt20190885